

# Preparation, proton conduction, and application in ammonia synthesis at atmospheric pressure of $\text{La}_{0.9}\text{Ba}_{0.1}\text{Ga}_{1-x}\text{Mg}_x\text{O}_{3-x}$

Cheng Chen · Guilin Ma

Received: 29 March 2008 / Accepted: 20 May 2008 / Published online: 7 June 2008  
© Springer Science+Business Media, LLC 2008

**Abstract**  $\text{La}_{0.9}\text{Ba}_{0.1}\text{Ga}_{1-x}\text{Mg}_x\text{O}_{3-x}$  ( $0 \leq x \leq 0.25$ ) was prepared by the microemulsion method. A single phase of  $\text{LaGaO}_3$  perovskite structure was formed when  $x$  was  $\geq 0.15$ . Electrochemical hydrogen permeation (hydrogen pumping) proved that  $\text{La}_{0.9}\text{Ba}_{0.1}\text{Ga}_{1-x}\text{Mg}_x\text{O}_{3-x}$  had proton conduction, and the proton conduction was measured by AC impedance spectroscopy method from 400 to 800 °C in hydrogen atmospheres. Among these samples,  $\text{La}_{0.9}\text{Ba}_{0.1}\text{Ga}_{0.8}\text{Mg}_{0.2}\text{O}_{3-x}$  has the highest proton conductivity with the values of  $9.51 \times 10^{-4}$  to  $4.68 \times 10^{-2} \text{ S cm}^{-1}$  at 400–800 °C. Ammonia was synthesized from nitrogen and hydrogen at atmospheric pressure in an electrolytic cell using  $\text{La}_{0.9}\text{Ba}_{0.1}\text{Ga}_{0.8}\text{Mg}_{0.2}\text{O}_{3-x}$  as electrolyte. The rate of  $\text{NH}_3$  formation was  $1.89 \times 10^{-9} \text{ mol s}^{-1} \text{ cm}^{-2}$  at 520 °C upon imposing a current of 1 mA through the cell.

## Introduction

In 1994, Ishihara reported that  $\text{Sr}^{2+}$ - and  $\text{Mg}^{2+}$ -doped  $\text{LaGaO}_3$  system exhibited high oxide ion conductivity, in particular, and oxide ion conductivity of  $\text{La}_{0.9}\text{Sr}_{0.1}\text{Ga}_{0.8}\text{Mg}_{0.2}\text{O}_{3-x}$  was higher than that of YSZ by an order of magnitude and its oxide ion transport number  $t_i$  was quite close to 1 over a wide range of oxygen partial pressures from 1 to  $10^{-20}$  atm [1]. Therefore, the doped  $\text{LaGaO}_3$  perovskite-type oxides are regarded as the promising candidate electrolytes for intermediate temperature fuel cells.

But their proton conduction was neglected by researchers except Goodenough in a long time. Goodenough reported that the conductivities of the cubic perovskite  $\text{La}_{0.9}\text{Sr}_{0.1}\text{Ga}_{0.8}\text{Mg}_{0.2}\text{O}_{3-x}$  were the same in dry air, ambient air, and water-saturated air; he came to a conclusion that there was no evidence of proton conduction in  $\text{Sr}^{2+}$ - and  $\text{Mg}^{2+}$ -doped  $\text{LaGaO}_3$  [2].

However, recently we discovered  $\text{LaGaO}_3$  doped with Sr on the La site and Mg/Zn on the Ga site,  $\text{La}_{0.9}\text{Sr}_{0.1}\text{Ga}_{0.8}\text{Mg}_{0.2}\text{O}_{3-x}$  and  $\text{La}_{0.9}\text{Sr}_{0.1}\text{Ga}_{0.9}\text{Zn}_{0.1}\text{O}_{3-x}$ , exhibited excellent proton conduction in  $\text{H}_2$  atmosphere and a mixed conduction of proton and oxide-ion in wet air atmosphere [3–6].

The conventional synthesis method for  $\text{LaGaO}_3$ -based oxides is the solid-state reaction method. Although this method is simple and straightforward, an impure phase, which is associated with poor component distribution, usually exists in these oxides [7]. Therefore, some liquid-phase methods, such as sol-gel, co-precipitation, the Pechini method or hydrothermal reaction [8–12], were employed to prepare  $\text{LaGaO}_3$ -based ceramics due to the advantages of higher component homogeneity and phase purity and lower sintering temperature of the powders compared with the solid-state reaction method.

In this study, an important series in  $\text{LaGaO}_3$ -based perovskite-type oxide family,  $\text{La}_{0.9}\text{Ba}_{0.1}\text{Ga}_{1-x}\text{Mg}_x\text{O}_{3-x}$  ( $0 \leq x \leq 0.25$ ), was prepared by a reverse microemulsion method (W/O), and its proton conduction was investigated via various electrochemical methods in the intermediate temperature range of 400–800 °C.

Ammonia synthesis at atmospheric pressure became one of the important applications of proton conductor since it was synthesized successfully using  $\text{SrCe}_{0.95}\text{Yb}_{0.05}\text{O}_{3-x}$  as the electrolyte by Marnellos and Stoukides [13]. In this study, perovskite-type oxides,  $\text{La}_{0.9}\text{Ba}_{0.1}\text{Ga}_{0.8}\text{Mg}_{0.2}\text{O}_{3-x}$

C. Chen · G. Ma (✉)  
Key Laboratory of Organic Synthesis of Jiangsu Province,  
School of Chemistry and Chemical Engineering,  
Suzhou University, Suzhou 215123, China  
e-mail: 32uumagl@suda.edu.cn

prepared by the microemulsion method, were tested as electrolytes in the synthesis of ammonia at atmospheric pressure.

## Experimental

All the reagents used are analytical-grade. The preparation of precursors of samples is as follows. The microemulsion, A, was confected. The required amounts of  $\text{La}(\text{NO}_3)_3$ ,  $\text{Ba}(\text{NO}_3)_2$ ,  $\text{Ga}(\text{NO}_3)_3$ , and  $\text{Mg}(\text{NO}_3)_2$  were dissolved in distilled water by stirring to obtain a nitrate solution. The required amounts of hexadecyltrimethylammoniumbromide (4 g) as surfactants and *n*-butanol (150 mL) were added to cyclohexane (80 mL) as oil phase, and then the above nitrate solution was added and stirred unto transparency. The microemulsion, B, was confected in a similar way. An aqueous solution of  $(\text{NH}_4)_2\text{CO}_3\text{-NH}_4\text{OH}$  as coprecipitation reagent was added to a mixed solution of hexadecyltrimethylammoniumbromide (4 g), *n*-butanol (150 mL), and cyclohexane (80 mL). Then, the microemulsion B was dripped to microemulsion A by stirring at 60 °C. The resulted white precipitate precursors were filtrated and dried.

The precursors were pressed into discs and calcined at 1000 °C for 5 h in air. The calcined discs were crushed and milled into powder and again pressed into discs. The calcining and milling processes were repeated twice. Finally, the powders were pressed into pellets (diameter 20 mm, thickness 2 mm) by a hydrostatic pressure  $2.5 \times 10^8$  Pa, and the pellets were sintered from 1350 to 1430 °C for 10 h in air.

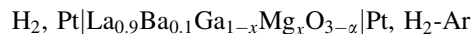
Transmission electron microscopy (TEM) FEI Tecnai G<sup>2</sup> 20 was used to characterize the precursors of samples. Differential scanning calorimetry and thermogravimetric analysis (DSC-TGA) was carried out in air atmosphere from 0 to 1000 °C by 2960 SDT V3.0F thermal analysis instrument with a ramp rate of 20 °C min<sup>-1</sup> and 3 mg powder. The phase analysis of the sintered samples was carried out by the powder X-ray diffraction (XRD) method using a Rigaku D/MAX-IIIC X-ray diffractometer with Cu K $\alpha$  radiation. The diffraction patterns were obtained at room temperature in the  $2\theta$  range of 20–80°. The step size and the scan rate were set at 0.0167° and 2.00° min<sup>-1</sup>, respectively.

The electrochemical measurements were conducted using the ceramic pellets (diameter 16 mm, thickness 0.6 mm) as electrolytes and porous platinum as electrode material in the temperature range of 400–800 °C. The ceramic samples were sealed into a mullite tube with a molten Pyrex glass in the homemade furnace.

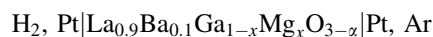
The electrical conductivity of the ceramic samples was measured by AC impedance method in H<sub>2</sub> atmosphere over

the frequency range 1 Hz to 3 MHz using electrochemical workstations (Zahner IM6EX).

To estimate the contribution of ion to the conduction, the electromotive force (EMF) of the following hydrogen concentration cell was measured:

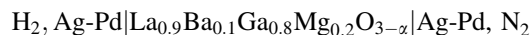


To confirm the proton conduction in  $\text{La}_{0.9}\text{Ba}_{0.1}\text{Ga}_{1-x}\text{Mg}_x\text{O}_{3-x}$  directly, the electrochemical hydrogen permeation (hydrogen pumping) through the ceramics was conducted by imposing a direct current on the electrolytic cell:



Pure hydrogen gas at 1 atm was supplied to the anode chambers of the above cells. For the hydrogen concentration cell, the partial pressure of hydrogen gas in the cathode chamber,  $p_{\text{H}_2}$ , was controlled by mixing hydrogen and argon using a gas blender. For the hydrogen pump, the argon gas in cathode chamber was dried by the steam above liquid nitrogen (about -115 °C) and a direct current was sent to the electrolytic cell. The EMF of hydrogen concentration cell and the rate of hydrogen permeation (hydrogen pumping) were measured.

Ammonia was synthesized in an electrolytic cell as the following:



The catalyst surface area of the Ag-Pd electrode was 1.13 cm<sup>-2</sup>. NH<sub>3</sub> was adsorbed by 10 mL of dilute sulfuric acid with an initial pH of 3.23 for 30 min. The cathode and the anode were fed with a dry high pure nitrogen stream (99.999%, flow rate: 30 mL min<sup>-1</sup>, dried by the steam above liquid nitrogen) and high pure hydrogen stream (99.999%, flow rate: 30 mL min<sup>-1</sup>), respectively. The effects of operating temperature and applied current on the rate of ammonia formation were investigated. The concentration of NH<sub>4</sub><sup>+</sup> in the absorption solution was analyzed by using the Nessler's reagent and spectrophotometry [6]. The blank test was also performed under open circuit condition.

## Results and discussion

A typical TEM image of precursor of sample prepared by the microemulsion method is shown in Fig. 1. The precursor appears to be spheres with a narrow size distribution of about 40–50 nm and without serious agglomeration. This is mainly determined by structural properties of the microemulsion system. In the mixed microemulsion of the microemulsion A and B, the well-dispersed aqueous droplets in the oil phase could act as microreactors. A

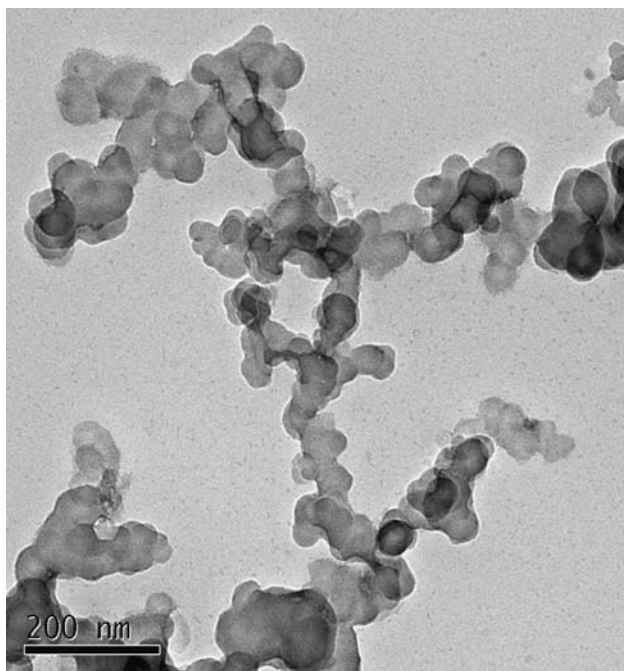


**Fig. 1** A typical TEM image of precursor of sample prepared by the microemulsion method

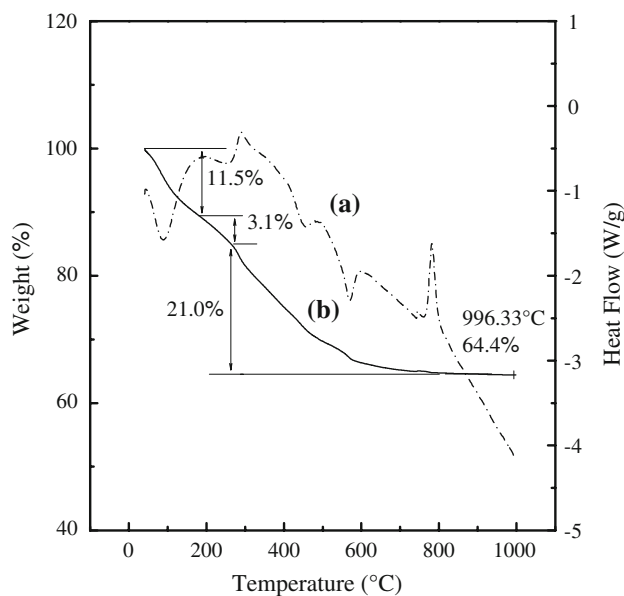


**Fig. 2** DSC (a) and TGA (b) analysis for precursor of sample prepared by the microemulsion method

precipitation reaction could occur only within the droplets, resulting in the formation of uniform spherical particles.

A representative of DSC and TGA analysis for precursor of sample is displayed in Fig. 2. Curve (a) shows DSC results, while curve (b) shows TGA results. The drop of weight from 0 to 190 °C is mostly due to the loss of water. The drop in the weight from 88.5 to 85.4% in temperature range of 190–250 °C is most likely due to decomposition

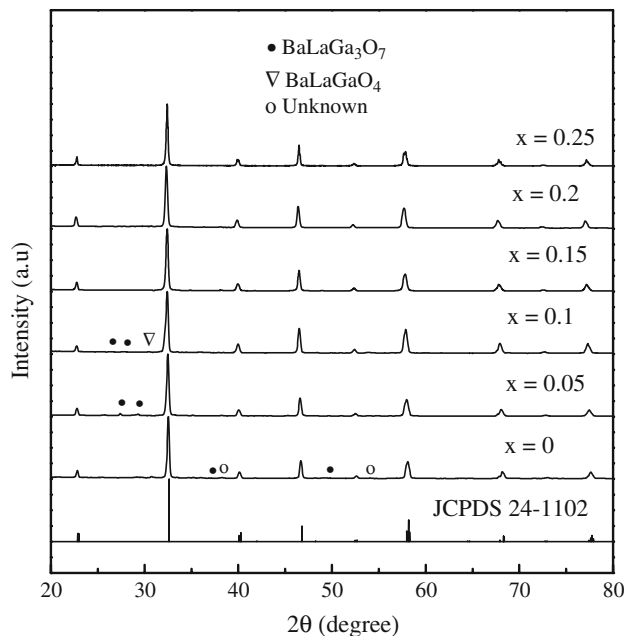
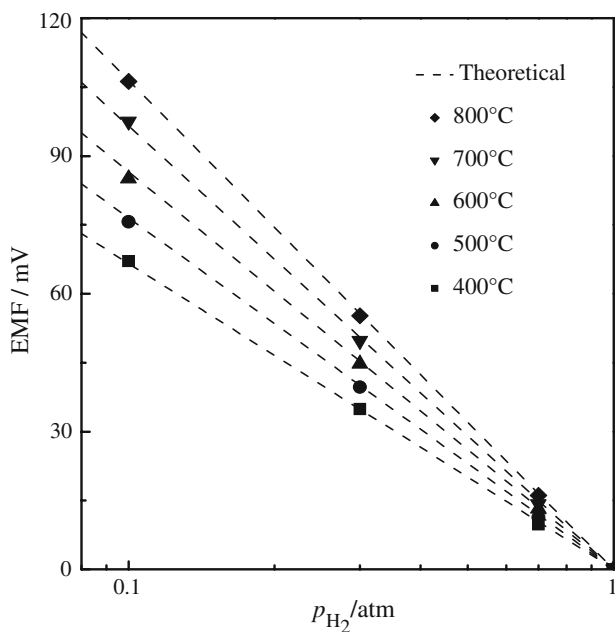


**Fig. 3** Powder XRD patterns of  $\text{La}_{0.9}\text{Ba}_{0.1}\text{Ga}_{1-x}\text{Mg}_x\text{O}_{3-x}$  ( $0 \leq x \leq 0.25$ ) prepared by the microemulsion method

of residual organic component. The rapid drop in weight from 85.4 to 64.4% in the temperature range of 250–800 °C is consistent with the DSC peak at about 780 °C, which is probably due to the transformation of the material to the  $\text{La}(\text{Ba})\text{Ga}(\text{Mg})\text{O}_3$  perovskite phase. Above 800 °C, the sample hardly loses weight with increasing temperature further. In order to obtain better sintered samples, 1000 °C is selected as calcining temperature.

Figure 3 shows the powder XRD patterns of  $\text{La}_{0.9}\text{Ba}_{0.1}\text{Ga}_{1-x}\text{Mg}_x\text{O}_{3-x}$  ( $0 \leq x \leq 0.25$ ) prepared via the microemulsion method. The second phases ( $\text{BaLaGa}_3\text{O}_7$  and  $\text{BaLaGaO}_4$  [14]) besides the main phase  $\text{LaGaO}_3$  (JCPDS 24-1102) were detected in all specimens except  $\text{La}_{0.9}\text{Ba}_{0.1}\text{Ga}_{1-x}\text{Mg}_x\text{O}_{3-x}$  ( $0.15 \leq x \leq 0.25$ ); that is, the samples have already formed a single phase of  $\text{LaGaO}_3$  perovskite structure when  $x$  is  $\geq 0.15$ . Lee et al. reported that  $\text{La}_{0.9}\text{Ba}_{0.1}\text{Ga}_{1-x}\text{Mg}_x\text{O}_{3-x}$  prepared by the solid-state reaction method formed a single phase when  $x$  was  $\geq 0.2$  [14, 15]. It is obvious that the microemulsion method is superior to the conventional solid-state reaction method, which may be due to its advantage of good dispersion, the size of particles in nanometer grade (shown in Fig. 1), and higher component homogeneity and purity of powder.

The relationship between the EMFs of hydrogen concentration cell and the hydrogen partial pressure,  $p_{\text{H}_2}$ , in the temperature range of 400–800 °C, using  $\text{La}_{0.9}\text{Ba}_{0.1}\text{Ga}_{0.8}\text{Mg}_{0.2}\text{O}_{3-x}$  as electrolyte, is displayed in Fig. 4. The dotted line stands for the theoretical EMF ( $E_{\text{cal}}$ ) calculated from Nernst equation at each temperature. The solid symbols stand for the observed EMFs ( $E_{\text{obs}}$ ). As shown in



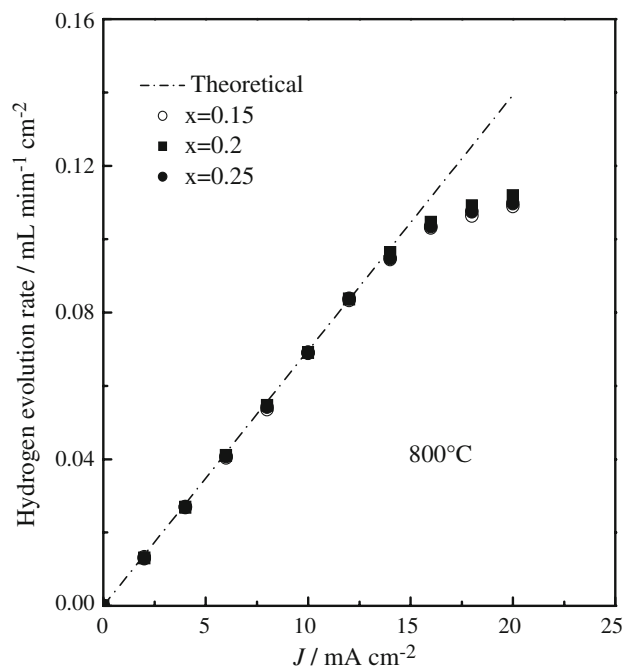
**Fig. 4** EMFs of hydrogen concentration cell:  $\text{H}_2$ ,  $\text{Pt}|\text{La}_{0.9}\text{Ba}_{0.1}\text{Ga}_{0.8}\text{Mg}_{0.2}\text{O}_{3-x}|\text{Pt}$ ,  $\text{H}_2$ -Ar

Fig. 4, each  $E_{\text{obs}}$  was nearly equal to the corresponding  $E_{\text{cal}}$ , and the relationship between the  $E_{\text{obs}}$  and the logarithm of  $p\text{H}_2$  was linear. This indicates  $\text{La}_{0.9}\text{Ba}_{0.1}\text{Ga}_{0.8}\text{Mg}_{0.2}\text{O}_{3-x}$  in hydrogen atmosphere was pure ion conductor from 400 to 800 °C, and the ionic transport number,  $t_i$ , determined from  $E_{\text{obs}}/E_{\text{cal}} = t_i$ , was almost unity. Similar results can be obtained when using other samples as electrolytes.

In order to prove the proton conduction in the samples directly, the electrochemical hydrogen permeation (hydrogen pumping) of the samples was performed. The concentration of hydrogen evolved in the cathode compartment was detected by a hydrogen detector, and the hydrogen evolution rate  $v$  was calculated by the following equation.

$$v = \frac{273.15 \cdot V_{\text{Ar}} \cdot x}{(273.15 + T) \cdot S}$$

where  $V_{\text{Ar}}$  is the flow rate of carrier gas (Ar),  $x$  is the concentration of the generated hydrogen gas in mixed gas,  $T$  is surrounding temperature, and  $S$  is the area of the cathode. In the equation,  $V_{\text{Ar}} \cdot x/S$  is the hydrogen evolution rate at the surrounding temperature  $T$ , and it is converted into the hydrogen evolution rate  $v$  at the standard state (temperature: 0 °C, pressure:  $1.01 \times 10^{-5}$  Pa) through the equation. The theoretical rate (standard state) can be calculated from Faraday's law. The representative results are shown in Fig. 5. It can be seen that the hydrogen evolution rate well coincided with the theoretical one in the lower current density region ( $J < 13 \text{ mA cm}^{-2}$ ). This indicates



**Fig. 5** Hydrogen evolution rate versus applied current density  $J$  at 800 °C. Dotted line shows the theoretical value calculated from Faraday's law, assuming that the sample is a pure proton conductor. Thickness of the electrolyte is 0.6 mm

that the charge carriers in the sample are protons in hydrogen atmosphere, that is,  $\text{La}_{0.9}\text{Ba}_{0.1}\text{Ga}_{1-x}\text{Mg}_x\text{O}_{3-x}$  is proton conductor in hydrogen atmosphere, and the ionic transport number  $t_i \approx 1$  obtained from Fig. 4 represents protonic. On the other hand, the hydrogen evolution rate deviated from the theoretical value in the higher current density range ( $J > 13 \text{ mA cm}^{-2}$ ). The origin of this deviation is not clear yet. It may be relevant to the electrode polarization and presence of some electronic conductivity in the samples under this condition [3].

Figure 6 shows the dependence of the conductivities for  $\text{La}_{0.9}\text{Ba}_{0.1}\text{Ga}_{1-x}\text{Mg}_x\text{O}_{3-x}$  series with the Mg dopant content in hydrogen atmosphere at 400–800 °C. As already confirmed above,  $\text{La}_{0.9}\text{Ba}_{0.1}\text{Ga}_{1-x}\text{Mg}_x\text{O}_{3-x}$  is a proton conductor in hydrogen atmosphere, so the conductivities of  $\text{La}_{0.9}\text{Ba}_{0.1}\text{Ga}_{1-x}\text{Mg}_x\text{O}_{3-x}$  shown in Fig. 6 in hydrogen atmosphere are protonic. The highest conductivity is observed for the sample of  $x = 0.2$  with values of  $9.51 \times 10^{-4}$  to  $4.68 \times 10^{-2} \text{ S cm}^{-1}$  at 400–800 °C, which is an order of magnitude higher than that of the sample of  $x = 0$ , and decreases as the Mg dopant content increases further. This can be explained according to defect chemistry. Under the same doping level of  $\text{Ba}^{2+}$  at  $\text{La}^{3+}$  sites, the concentration of point defects  $\text{Mg}_{\text{Ga}}'$  and oxygen vacancy  $\text{V}_{\text{O}}^{\bullet\bullet}$  increases as the doping level of  $\text{Mg}^{2+}$  at  $\text{Ga}^{3+}$  sites increases, as described by the following defect reaction using Kroger–Vink notation.

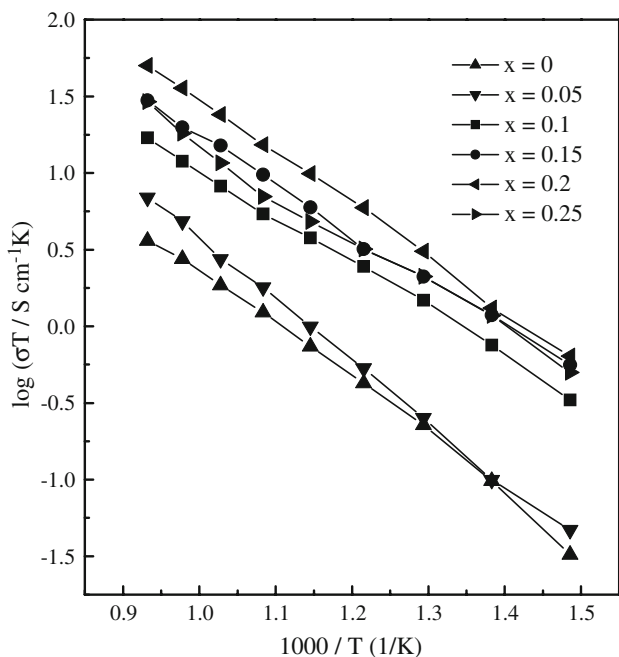
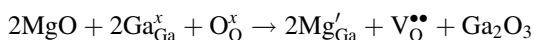
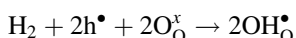
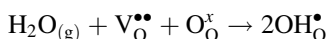


**Fig. 6** The conductivity of  $\text{La}_{0.9}\text{Ba}_{0.1}\text{Ga}_{1-x}\text{Mg}_x\text{O}_{3-x}$  ( $0 \leq x \leq 0.25$ ) in hydrogen atmosphere, measured by AC impedance



In the atmosphere containing vapor or hydrogen, the defect reactions concerning the proton dissolution can be depicted as follows.



where  $\text{OH}_{\text{O}}^{\bullet}$  indicates the OH group at the oxygen site. The proton conduction can be attributed to hopping of protons among the neighbors of the oxygen ions [16, 17]. Obviously, the concentration of  $\text{OH}_{\text{O}}^{\bullet}$  increases with the increase of concentration of  $\text{V}_{\text{O}}^{\bullet\bullet}$  resulting from substituting  $\text{Mg}^{2+}$  for  $\text{Ga}^{3+}$  sites. Therefore the conductivities increase with increasing doping level of  $\text{Mg}^{2+}$ . However, at the same time, the concentration of point defect pairs ( $\text{Mg}'_{\text{Ga}} - \text{V}_{\text{O}}^{\bullet\bullet}$ ) and ( $\text{Mg}'_{\text{Ga}} - \text{OH}_{\text{O}}^{\bullet}$ ), which result from the coulombic attraction existing among the point defects with opposite charges, increases also with increasing doping level of  $\text{Mg}^{2+}$  at  $\text{Ga}^{3+}$  sites, leading to the decrease in proton conductivity when the doping level of  $\text{Mg}^{2+}$  is more than 20 at.%.

Ammonia was synthesized in an electrolytic cell using  $\text{La}_{0.9}\text{Ba}_{0.1}\text{Ga}_{0.8}\text{Mg}_{0.2}\text{O}_{3-x}$  as an electrolyte. The blank test under open circuit conditions (imposed current was zero) demonstrated no ammonia was detectable under these conditions. Figure 7 shows the relationship between the rate of ammonia formation and operating temperature. A direct current (1 mA) was applied to the cell for ammonia synthesis. It can be seen that the rate of ammonia formation

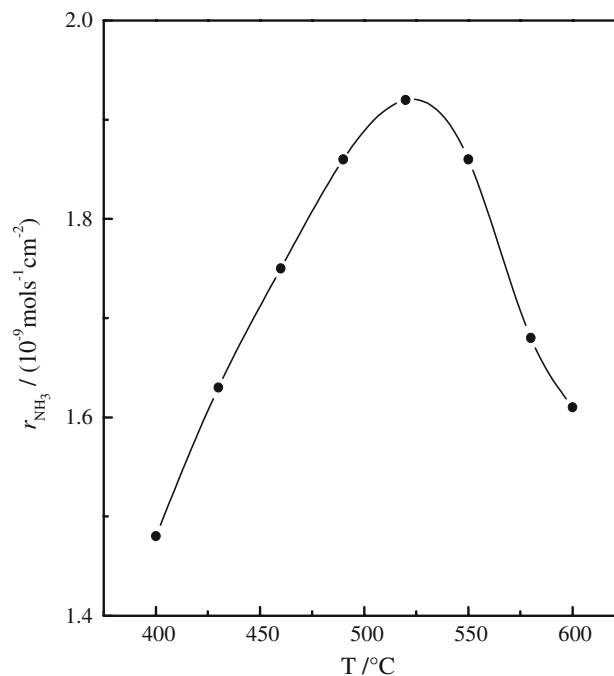


**Fig. 7** The relationship between the rate of ammonia formation and operating temperature. The electrolytic cell was:  $\text{H}_2, \text{Ag-Pd}|\text{La}_{0.9}\text{Ba}_{0.1}\text{Ga}_{0.8}\text{Mg}_{0.2}\text{O}_{3-x}|\text{Ag-Pd}, \text{N}_2$  the applied direct current through the cell was 1 mA

increases with the increasing temperature in the range from 400 to 520 °C, and then decreases as temperature increases further. The maximum rate of ammonia formation appears at 520 °C, which is the optimum temperature for ammonia synthesis in this study. This is because the rate of ammonia formation depends not only on proton conductivity, volumetric flow rate of  $\text{H}_2$  and  $\text{N}_2$ , and current, but also on the rate of  $\text{NH}_3$  decomposition. The proton conductivity of the sample increases with the increase of temperature, which may help in ammonia formation, but at the same time, the rate of  $\text{NH}_3$  decomposition also increases [18].

The effect of applied current on the rate of ammonia formation at 520 °C is shown in Fig. 8. As can be seen, the rate of ammonia formation increases with increasing applied current, then increased slightly after 1 mA. It was concluded that 1 mA was the optimum current for synthesizing ammonia in this study. The rate of  $\text{NH}_3$  formation is  $1.89 \times 10^{-9} \text{ mol s}^{-1} \text{ cm}^{-2}$  when current is 1 mA. As mentioned above, protonic transport number of  $\text{La}_{0.9}\text{Ba}_{0.1}\text{Ga}_{0.8}\text{Mg}_{0.2}\text{O}_{3-x}$  is almost unity. Therefore, the ratio  $I/2F$  is equal to the electrochemical molar flux of hydrogen through the sample and the maximum amount of  $\text{NH}_3$  formation should be  $2/3 \times I/2F$  [13]. The molar flux of hydrogen through the sample is  $4.59 \times 10^{-9} \text{ mol s}^{-1} \text{ cm}^{-2}$  and the theoretical maximum amount of  $\text{NH}_3$  formation should be  $3.06 \times 10^{-9} \text{ mol s}^{-1} \text{ cm}^{-2}$  when the imposed current is 1 mA. The ratio of the practical rate of ammonia formation



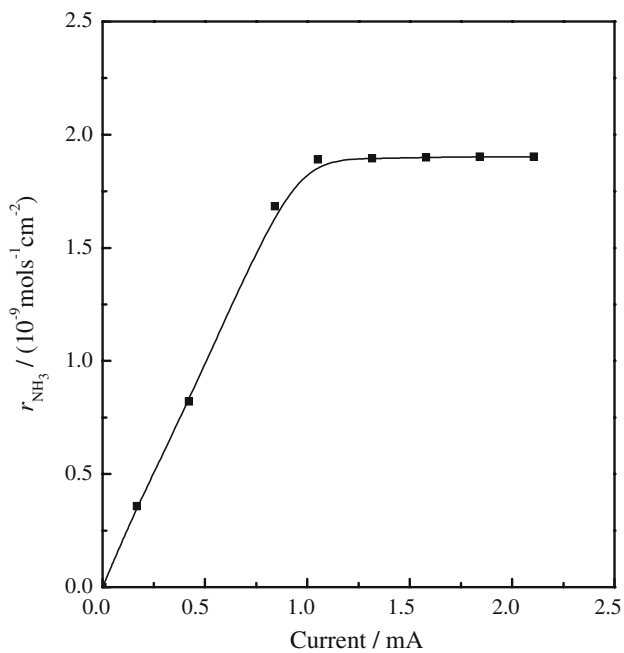


**Fig. 8** The effect of applied current on the rate of ammonia formation at 520 °C,  $\text{La}_{0.9}\text{Ba}_{0.1}\text{Ga}_{0.8}\text{Mg}_{0.2}\text{O}_{3-x}$  as electrolyte

to the theoretical one is above 60%. The low rate of ammonia formation and efficiency in this study may be relevant to (i) very small catalyst surface area of the Ag-Pd electrode [19], (ii) the activation of catalyst, (iii) the rate of ammonia decomposition [18], (iv) the thickness of electrolyte, and (v) the electrode polarization. The optimized conditions for ammonia synthesis still need to be investigated.

On the other hand, ammonia synthesis was performed successfully and proved that  $\text{La}_{0.9}\text{Ba}_{0.1}\text{Ga}_{0.8}\text{Mg}_{0.2}\text{O}_{3-x}$  has proton conduction in hydrogen atmosphere.

## Conclusions

A series of ceramic samples,  $\text{La}_{0.9}\text{Ba}_{0.1}\text{Ga}_{1-x}\text{Mg}_x\text{O}_{3-x}$  ( $0 \leq x \leq 0.25$ ), were prepared by a microemulsion method. The samples with  $0.15 \leq x \leq 0.25$  are of a single phase of  $\text{LaGaO}_3$  perovskite structure, indicating that the microemulsion method is superior to a conventional solid-state reaction method in this study. The samples of  $0 \leq x \leq 0.25$  showed almost pure proton conductors in

hydrogen atmosphere from 400 to 800 °C.  $\text{La}_{0.9}\text{Ba}_{0.1}\text{Ga}_{0.8}\text{Mg}_{0.2}\text{O}_{3-x}$  has the highest proton conductivity with values of  $9.51 \times 10^{-4}$  to  $4.68 \times 10^{-2} \text{ S cm}^{-1}$  at 400–800 °C among the samples of  $0 \leq x \leq 0.25$ . The ammonia synthesis at atmospheric pressure in an electrolytic cell using  $\text{La}_{0.9}\text{Ba}_{0.1}\text{Ga}_{0.8}\text{Mg}_{0.2}\text{O}_{3-x}$  as an electrolyte was carried out successfully. This provided a further evidence of proton conduction in  $\text{La}_{0.9}\text{Ba}_{0.1}\text{Ga}_{0.8}\text{Mg}_{0.2}\text{O}_{3-x}$ .

**Acknowledgement** This work was supported by the National Natural Science Foundation of China (No. 20771079).

## References

- Ishihara T, Matsuda H, Takita Y (1994) J Am Chem Soc 116:3801. doi:10.1021/ja00088a016
- Feng M, Goodenough JB (1994) Eur J Solid State Inorg Chem 31:663
- Ma G, Zhang F, Zhu J, Meng G (2006) Chem Mater 18:6006. doi:10.1021/cm0612954
- Zhang F, Sun L, Zhu J et al (2008) J Mater Sci 43:1587. doi:10.1007/s10853-007-2328-9
- Zhu JL, Zhang F, Chen C et al (2007) Chin J Inorg Chem 23:1621
- Zhang F, Yang Q, Pan B et al (2007) Mater Lett 61:4144. doi:10.1016/j.matlet.2007.01.060
- Marnellos E, Labeau M (1998) J Eur Ceram Soc 18:1397. doi:10.1016/S0955-2219(98)00016-8
- Zhang J, Wen Z, Han J et al (2007) J Alloys Compd 440:270. doi:10.1016/j.jallcom.2006.09.016
- Brunckova H, Medvecký L, Mihalik J (2008) J Eur Ceram Soc 28:123. doi:10.1016/j.jeurceramsoc.2007.09.026
- Navale SC, Samuel V, Gaikwad AB et al (2007) Ceram Int 33:297. doi:10.1016/j.ceramint.2005.08.012
- Lemos FCD, Melo DMA, Silva da JEC (2005) Mater Res Bull 40:187. doi:10.1016/j.materresbull.2004.08.010
- Athawale AA, Chandwadkar A, Karandikar P et al (2005) Mater Sci Eng B 119:87. doi:10.1016/j.mseb.2005.01.007
- Marnellos G, Stoukides M (1998) Science 282:98. doi:10.1126/science.282.5386.98
- Choi SM, Lee KT, Lee HL et al (2000) Solid State Ionics 131:221. doi:10.1016/S0167-2738(00)00673-1
- Kim S, Chun MC, Lee KT et al (2001) J Power Sources 93:279. doi:10.1016/S0378-7753(00)00567-X
- Mather GC, Islam MS (2005) Chem Mater 17:1736. doi:10.1021/cm047976l
- Sata N, Hiramoto K, Ishigame M et al (1996) Phys Rev B 54:15795. doi:10.1103/PhysRevB.54.15795
- Li ZJ, Liu RQ, Xie YH et al (2005) Solid State Ionics 176:1063. doi:10.1016/j.ssi.2005.01.009
- Wang JD, Xie YH, Li RQ et al (2005) Mater Res Bull 40:1294. doi:10.1016/j.materresbull.2005.04.008